ANN-based Reliability Enhancement of SMPS Aluminium Electrolytic Capacitors in Cold Environments

Sunwoo Jeong , Akeem Bayo Kareem , Sungwook Song , Jang-Wook Hur *

Posted Date: 20 July 2023

doi: 10.20944/preprints202307.1373.v1

Keywords: aluminium electrolytic capacitors; artificial neural networks; cold experiment; Pearson correlation coefficient; switched mode power supply

Article

ANN-Based Reliability Enhancement of SMPS Aluminium Electrolytic Capacitors in Cold Environments

Sunwoo, Jeong [2], Akeem Bayo Kareem [2], Sungwook Song [1] and Jang-Wook Hur [2,*]

[1] Department of Mechanical Engineering, Kumoh National Institute of Technology, Republic of Korea
[2] Department of Aeronautics, Mechanical and Electronic Convergence Engineering, Kumoh National Institute of Technology, 61 Daehak-ro, Gumi-si 39177, Republic of Korea

Abstract: Switched-mode power supplies (SMPS) often utilize electrolytic capacitors due to their substantial energy density and economical pricing. However, their ability to function at low temperatures is essential for dependable operation in several sectors, including telecommunications, automotive, and aerospace. This study includes an experimental evaluation of how well standard SMPS electrolytic capacitors operate at low temperatures. This paper investigates the suitability of standard electrolytic capacitors used in switched-mode power supplies (SMPS) for low-temperature applications. The experimental evaluation exposed the capacitors to temperatures ranging from - 5 °C to - 40 °C, assessing capacitance (Cp), impedance (Z), dissipation factor (DF), and equivalent series resistance (ESR) at each temperature. The capacitor's time-domain electrical signals were analyzed using the Pearson correlation coefficient to extract discriminative features. These features were input into an Artificial Neural Network (ANN) for training and testing. Results indicated a significant impact of low temperatures on capacitor performance. Capacitance decreased with lower temperatures, while ESR and leakage current increased, affecting stability and efficiency. Impedance proved to be a valuable diagnostic tool for identifying potential capacitor failure, showing a 98.44% accuracy drop at - 5 degrees and 88.75% at the peak temperature, indicating proximity to the manufacturer's specified limit. The study suggests further research and development to improve electrolytic capacitors' performance in SMPS systems under cold conditions to enhance efficiency and reliability.

Keywords: aluminium electrolytic capacitors; artificial neural networks; cold experiment; Pearson correlation coefficient; switched mode power supply

1. Introduction

Aluminium electrolytic capacitors (AEC) are vital in efficiently operating switched-mode power supplies (SMPS) by providing energy storage and voltage regulation. These capacitors are widely used due to their high capacitance and cost-effectiveness. However, their performance at low temperatures is a critical aspect that demands a thorough investigation, particularly in applications where SMPS are subjected to sub-zero operating conditions. Understanding the behaviour of aluminium electrolytic capacitors in such environments is essential to ensure power supply systems' reliable and stable performance in a wide range of operating conditions [1–4]. The low-temperature performance of aluminium electrolytic capacitors can be significantly affected by various factors, including temperature-dependent capacitance, leakage current, and the impact on overall power supply efficiency. The capacitor's characteristics can deviate from their nominal values at low temperatures, leading to degraded performance and potential failure. This is particularly important in aerospace, automotive, and telecommunications applications, where SMPS are exposed to extreme temperature variations [10,12]. Despite the significance of low-temperature performance, more comprehensive experimental investigations need to focus specifically on aluminium electrolytic capacitors in SMPS. Most existing studies in the field have primarily concentrated on the behaviour of other capacitors or have explored

 doi:10.20944/preprints202307.1373.v1

the impact of temperature on capacitors without delving into the specific nuances of aluminium electrolytic capacitors in SMPS applications [11].

Cold experiments have been conducted to study the impact of low temperatures on aluminium electrolytic capacitors. It has been observed that cold environments can significantly affect the performance and reliability of these capacitors. One prominent effect is the decrease in capacitance at lower temperatures. The dielectric oxide layer on the aluminium anode tends to thicken, reducing the effective surface area and decreasing capacitance [5–8]. Additionally, the capacitors' equivalent series resistance (ESR) tends to increase in cold conditions, impacting their overall impedance characteristics. Furthermore, the mechanical integrity of aluminium electrolytic capacitors can be compromised in cold environments. The contraction and expansion of the aluminium can and sealing materials due to temperature changes can induce mechanical stress, leading to potential damage and reduced reliability. Long-term exposure to low temperatures can also degrade the performance and reliability of aluminium electrolytic capacitors. Ageing tests conducted under cold conditions have shown a deterioration in their electrical properties and decreased operational lifespan. Research has examined different approaches, like fine-tuning electrolyte compositions, employing cold-temperature electrolytes, and enhancing packaging designs to augment the efficiency and dependability of aluminium electrolytic capacitors in chilly conditions. These efforts aim to mitigate the adverse effects of low temperatures and ensure the reliable operation of these capacitors in cold applications. Understanding the effects of cold temperatures on aluminium electrolytic capacitors is crucial for designing and operating systems in cold environments [9,33].

This research paper aims to bridge this gap by presenting an in-depth experimental investigation into the low-temperature performance of aluminium electrolytic capacitors in SMPS. The study will encompass various critical aspects, including capacitance variation, leakage current behaviour, equivalent series resistance (ESR), and the overall impact on the efficiency of the power supply system. By systematically analyzing the performance of aluminium electrolytic capacitors in different low-temperature scenarios, this research will contribute to developing guidelines and design considerations for engineers and researchers working on SMPS applications operating in extreme temperature environments. The achievements of this research paper are outlined as follows:

- This research paper introduces a statistical-based approach for extracting meaningful information from the dataset related to the aluminium electrolytic capacitor. This approach allows for the identification and analysis of key parameters that affect the capacitor's reliability.
- This research paper proposes the utilization of an ANN-based machine learning algorithm. The extracted meaningful information from the dataset is fed into the ANN to develop a predictive model for assessing the reliability of the capacitor. This algorithm enhances the accuracy of reliability predictions and aids in identifying potential failure modes.
- This research paper describes an experimental process that employs a data-driven and multi-choice approach for collecting various parameters related to the aluminium electrolytic capacitor. Parameters such as Equivalent Series Resistance (ESR), Dissipation Factor, Capacitance, and Impedance are measured using the HIOKI LCR Meter, providing a comprehensive dataset for analysis.
- The multi-choice approach implemented during the experimental process ensures the collection of diverse data points for different capacitor parameters. This extensive dataset enhances the accuracy and robustness of the subsequent analysis and modelling.
- The collected dataset is subjected to in-depth analysis to identify correlations, patterns, and trends among the various parameters. This analysis helps uncover the key factors influencing the reliability of the aluminium electrolytic capacitor.
- Leveraging the statistical-based approach and the ANN algorithm, a predictive model is developed to assess the reliability of the capacitor. The model takes into account the interrelationships among the collected parameters, enabling accurate reliability predictions.
- The research paper's contributions lead to an enhanced method for assessing the reliability of aluminium electrolytic capacitors used in SMPS. The combination of comprehensive dataset

 doi:10.20944/preprints202307.1373.v1

collection, statistical analysis, and machine learning algorithms results in more accurate and reliable predictions.

The rest of this research paper is as follows: Section 2 shows the literature and related works on the reliability of aluminium electrolytic capacitors applicable for SMPS. Section 3 summarises the theoretical background of the topics associated with the proposed model. Section 4 shows the breakdown of the data acquisition process inclusive of the parameters description of the whole experiment. Section 5 shows the deployed ANN-based model for capacitor reliability. Section 6 encompasses the entire derived result from the proposed model, while the research paper is concluded in Section 7.

2. Literature and Related Works

AECs are widely used in electrical and electronic applications due to their high capacitance, low cost, and robustness. They consist of an anode and a cathode separated by an electrolyte-soaked paper or polymer separator. The anode is formed by an aluminium foil with a thin oxide layer, which acts as the dielectric. The electrolyte facilitates ion movement, forming a stable oxide layer on the anode. Aluminium electrolytic capacitors offer high capacitance values and can handle high voltage ratings. They find applications in power supplies, audio equipment, motor drives, and many other electronic systems requiring energy storage and filtering capabilities. AECs typically consist of several layers. Starting from the outermost layer, a protective sleeve or coating provides insulation and mechanical protection. Beneath that is an anode foil made of high-purity aluminium, forming one electrode. The anode foil is covered with a dielectric layer, usually formed by an aluminium oxide film. The dielectric layer acts as the insulating material. Next, a paper or polymer separator is soaked in an electrolyte, facilitating ion movement. Finally, a cathode foil, typically aluminium, forms the second electrode. The tightly rolled or stacked layers ensure a compact structure with a high capacitance-to-volume ratio.

The papers provide different methods for studying and monitoring the condition of aluminium electrolytic capacitors. It presents a methodology for studying the impact of thermal cycling on the wear-out of aluminium electrolytic capacitors used in automotive cases [13]. It introduces an approach for investigating the influence of thermal cycling on the deterioration of aluminium electrolytic capacitors utilized in automotive applications [14]. It introduces a trial offline method for assessing the status of aluminium electrolytic capacitors through the estimation of equivalent series resistance and capacitance parameters [15]. It suggests an approach for determining the hotspot temperature of aluminium electrolytic capacitors using the linear relationship between capacitance and temperature [16]. This study presents a fault diagnostics framework for aluminium electrolytic capacitors in power supplies. Long-term frequency monitoring and statistical feature extraction were used to detect anomalies, achieving improved performance with increased data capacity. The k-nearest neighbours algorithm showed the highest accuracy (98.40%) and lowest computational cost [17]. This study focuses on monitoring electrolytic capacitors using a parameter observer (PO) to determine their equivalent capacity and serial resistance. The PO estimates the discharging circuit's time constant based on voltage measurements, enabling the calculation of the capacitor's parameters. Experimental results show that the proposed observer has faster error tracking than other methods, with the potential for real-time implementation due to its low computational requirements [18]. This paper introduces a data processing method using the box diagram technique to identify outliers in sensor data. Outliers are classified based on their persistence over time and linkage to other sensors. A clustering algorithm is employed for data reclassification. A risk coefficient is calculated using persistence and linkage, and a threshold is defined to differentiate between risk-specific and non-risk anomalies. A comprehensive evaluation model is established using quantitative scoring, principal component analysis, and 0,1 planning. The proposed evaluation method is evaluated objectively [19]. This research deals with the issue of identifying faults in squirrel cage induction motors (SCIMs) when operating under conditions of low load. By employing stator current information and an approach assisted by feature engineering, a technique for fault categorization is formulated using the support vector classification

 doi:10.20944/preprints202307.1373.v1

(SVC) algorithm. The method utilizes the Hilbert Transform and filter-based feature selection for precise fault categorization. The SVC exhibits remarkable diagnostic performance accuracy (97.32%) and surpasses alternative classifiers in accuracy and computation speeds [20]. This research centres on monitoring switch-mode AC/DC power supplies (SMPS) to identify issues in switching devices and capacitors. By utilizing dual sensing of current and voltage signals and applying statistically derived characteristics, an integrated approach is suggested for diagnosing system faults. The selection of features is carried out using correlation-based methods, and machine learning-based classifiers are utilized for fault detection and isolation (FDI). The outcomes demonstrate that random forest and gradient boosting classifiers are highly dependable but computationally demanding, whereas the decision tree classifier offers cost-effectiveness with reliable diagnostic results. The proposed framework is effective for diagnosing switching device issues and categorizing various states of the SMPS [21]. This research focuses on the significance of sturdy power converter designs and regulatory techniques in LED lighting setups. It introduces an innovative health assessment system that employs the brief duration least square Prony's method for identifying capacitor issues in a resilient LED driver. The setup enables constant monitoring of electrolytic capacitor status, averting complete system breakdown, and exhibits remarkable efficiency despite a restricted amount of data instances [22]. This research emphasizes the significance of preserving the robust functioning of capacitors in renewable energy generation setups. It suggests an unintrusive method for identifying faults using random forest classification to detect the critical level of aluminium electrolytic capacitors, eliminating the necessity for extra sensors in the converter [23]. Precise capacity assessment is vital for the secure and effective functioning of batteries. This research introduces an innovative approach to gauge the capacity of extensive LiFePO4 batteries, utilizing actual information obtained from electric vehicles. A comprehensive dataset from 85 cars is compiled, and a capacity prediction method that involves classification and aggregation is formulated. This technique combines a battery ageing trial with extensive data analysis to estimate even under diverse and authentic circumstances accurately. The suggested models, encompassing linear regression and neural networks, demonstrate dependable capacity prediction with minimal relative error. The effectiveness of these methodologies is confirmed through an ageing experiment, offering valuable insights for capacity estimation based on real-world data [24]. This article centres on temporal features and their importance in comprehending data patterns. The laborious manual extraction of features from extensive time-based datasets is time-consuming and demanding automation. The article introduces a correlation-dependent feature selection algorithm assessed on stress-predictive data, attaining superior classification accuracy (98.6%) in contrast to conventional statistical characteristics (67.4%). The research underscores the significance of analytical attributes over traditional statistical features for precise stress categorization [25]. The swift expansion in energy requirements compels the exploration of energy conservation. Demand flexibility (DF) initiatives and live meters (LM) offer crucial data for managing energy consumption on the consumer side. This research suggests cluster algorithms employing discrete wavelet transformation (DWT) to partition consumers according to their daily load patterns. The approach is deployed on the Manhattan dataset, demonstrating enhanced cluster efficiency and easing the analysis of electricity usage patterns [26].

With its abundant presence in the Vellore locality, Sunlight energy can be tapped using solar PV modules. A machine learning-based MPPT controller improves the PV array's effectiveness, ensuring ideal torque and steady speed for electric vehicles (EVs) under different load circumstances. The research employs a solar cell, SVPWM inverter, and DC-DC voltage booster to energize the EV, and the system's performance is assessed using MATLAB Simulink [27]. Microbe fuel cells (MFCs) transform organic substances into electric energy utilizing microorganisms, yet their limited power constrains their feasible use. This research utilizes machine learning techniques, encompassing support vector regression, artificial neural networks, and Gaussian process regression, to establish ideal data-informed models for MFCs. Fine-tuning hyperparameters through Bayesian, grid, and random exploration yields models with 99% precision for forecasting power density and output voltage, facilitating enhanced

Preprints (www.preprints.org) | NOT PEER-REVIEWED | Posted: 20 July 2023 doi:10.20944/preprints202307.1373.v1

MFC optimization [28]. This paper introduces a synthetic neural network-centred (SNN) energy management approach (SMA) for a hybrid AC/DC microgrid. It employs a dual-phase technique to ascertain the operational state and regulate the replenishment and release of the energy storage system. The microgrid integrated diverse converters and effectively functioned and governed with the suggested SNN-based EMA, as evidenced by empirical findings on a laboratory-scale setup [29]. Scientists have sought to enhance the effectiveness of photovoltaic systems (PVS) by forecasting weather conditions that influence PV module performance. This research suggests employing artificial neural networks (ANNs) to anticipate the PV system's temperature and radiation, utilizing JAYA-SMC hybrid control to identify the peak power point and duty cycle for a DC motor. The approach was proven exceptionally efficient, precisely assessing maximum power and stability for energy monitoring and control [30]. This article suggests a mixed AC/DC microgrid (MG) utilizing solar and wind renewable resources. The management of coordination and identification of faults are implemented to guarantee steadiness and equilibrium between generation and consumption and facilitate rapid fault localization and restoration. A proportional resonant (PR) current regulator lessens harmonics, while an artificial neural network (ANN) ensures precise fault detection. MATLAB simulation outcomes exhibit the efficiency of the suggested control approach in preserving stability, fulfilling load requirements, attaining energy equilibrium, and anticipating faults [31]. This research presents a modelling framework for a hybrid electric vehicle setup, emphasizing bidirectional DC-DC converters and coordinated regulation of energy sources. An artificial neural network (ANN) is implemented to optimize feedback control within the converter circuit to enhance traditional control techniques. The results indicate that the ANN controller significantly improves performance compared to conventional methods, as demonstrated through MATLAB/Simulink simulations. These simulations underscore the effectiveness of the ANN controller in diminishing steady-state error, peak overshoot, and settling time during both vehicle powering and regenerative braking modes [32]. These papers, as a whole, propose that the statistical feature engineering method and artificial neural network implementation can be utilised to monitor the status of aluminium electrolytic capacitors and forecast their lifespan and ensure their dependability.

3. Theoretical Backgrounds

3.1. Statistical Feature Engineering

The Pearson correlation coefficient (PCC) is a statistical metric that assesses the linear association between two variables. It is extensively employed in feature engineering and data analysis to comprehend the potency and orientation of the connection between variables. Often referred to as ρ, the Pearson correlation coefficient (PCC) varies between -1 and +1. A favourable value indicates a positive linear correlation, an adverse value indicates a negative linear correlation and a value of 0 indicates no linear correlation. [34,35]. The PCC between two variables, X and Y, can be mathematically expressed as follows:

$$\rho_{X,Y} = \frac{\mathrm{cov}(X,Y)}{\sigma_X \sigma_Y} \tag{1}$$

where σ_X and σ_Y are the standard deviations of X and Y, respectively, while $\mathrm{cov}(X,Y)$ is the covariance.

The PCC is calculated by taking the covariance of X and Y (the numerator) and dividing it by the product of their standard deviations (the denominator). The covariance measures how much the variables vary together, while the standard deviations measure the individual variability of each variable. The Pearson correlation coefficient has several important properties:

1. It is symmetric,
2. It is bounded between -1 and +1: The correlation coefficient cannot exceed these bounds,
3. It is sensitive to linear relationships: Although it may not account for nonlinear correlations, it quantifies the magnitude of the linear association between the two variables.

 doi:10.20944/preprints202307.1373.v1

In feature engineering, the PCC can be used to identify highly correlated variables or select features strongly correlated with the target variable in predictive modelling tasks. A high correlation between two features may indicate redundancy, suggesting that one can be dropped or combined with other features [36,37].

3.2. Artificial Neural Networks

The arrangement and operation of biological neural networks in the human brain provide inspiration for Artificial Neural Networks (ANNs). ANNs are composed of linked artificial neurons, nodes, or units arranged in layers. Every neuron receives inputs, conducts calculations, and generates an outcome. The links between neurons are linked to weights that ascertain the potency or significance of the connections. The mathematical expression for a single artificial neuron can be represented as follows:

$$y = f\left(\sum_{i=1}^{n} w_i \cdot x_i + b\right) \tag{2}$$

where:

- y is the output of the neuron,
- $f(\cdot)$ is the activation function that introduces non-linearity,
- w_i are the weights associated with the inputs,
- and b is the bias term.

The function $f(\cdot)$ brings non-linearity to the neuron's output, enabling the network to represent intricate connections in the data. Typical activation functions comprise the sigmoid, hyperbolic tangent (tanh), and rectified linear unit (ReLU). ANNs typically consist of three types of layers:

- Input Layer: The input data is acquired and transmitted to the subsequent layers. Each input node represents a characteristic or attribute of the input information.
- Hidden Layers: These intermediate neurons lie between the input and output layers. They execute calculations and modify the input across the network. The quantity of concealed neurons in the capacitor classifier algorithm and the number of neurons in each covert layer represent design decisions subject to variation based on the specific problem at hand.
- Output Layer: This layer generates the outcome of the network, which may encompass classification, regression, or any other preferred prognosis or result.

Training an ANN includes tuning the weights and biases of the neurons to diminish the disparity between the forecasted outcome of the network and the anticipated result. It is commonly accomplished through backpropagation, which employs optimization algorithms such as gradient descent to modify the weights according to the computed error. The mathematical expressions and theoretical foundations of ANNs extend beyond the individual neuron and into the architecture, training algorithms, and optimization techniques used to build and optimize neural networks. These concepts involve feedforward propagation, backpropagation, cost functions, gradient descent, regularization techniques, and more.

4. Data Acquisition Process

LCR (Inductance, Capacitance, and Resistance) meters are commonly used for data collection of electrical signals. These meters provide a convenient and accurate means of measuring the impedance characteristics of electronic components, such as resistors, capacitors, and inductors. LCR meters can accurately measure parameters like capacitance, inductance, resistance, quality factor (Q-factor), and equivalent series resistance (ESR). Connecting the electrical signal source or device under test to the LCR meter can measure and record the impedance response across a range of frequencies. This data collection process enables comprehensive analysis and characterization of the electrical

Preprints (www.preprints.org) | NOT PEER-REVIEWED | Posted: 20 July 2023 doi:10.20944/preprints202307.1373.v1

properties of components and circuits, facilitating design, troubleshooting, and quality control in various electronic applications. The experimental setup for the SMPS output capacitor is shown in Figure 1. Capacitor manufacturers specify nominal values based on IEC standards, defining capacitance for electrolytic capacitors. The researchers have ensured the measurement conditions align with the circuit's operational frequency, as capacitance fluctuates significantly with frequency. The experimental process conditions are described in Table 1, showing the set parameters to acquire the selected electrical signals. The LCR meter utilizes mathematical equations to measure the selected electrical signals, such as capacitance, impedance, dissipation factor, and equivalent series resistance (ESR). The equations are expressed in Table 2.

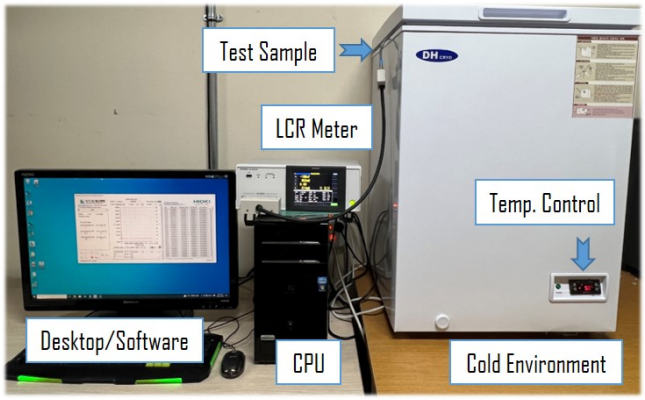

Figure 1. Experiment Setup for the SMPS Output Capacitor Data-Driven Process

Table 1. AEC Experimental Setup Conditions.

Functions	Description
Electrical Parameters	Cp–Z–D–Rs
Signal Level	0.5 Vrms
Total Frequency/Step	8 MHz/100 Hz
DC Bias	ON 1.0 volts
LowZ mode	ON
Measurement Range	Auto
Speed	SLOW2

Table 2. Electrical Signal and its Function.

Parameters	Definition	Functions
Cp	Capacitance	$Cp = \frac{D}{\omega R}$
Z	Impedance	$Z = \frac{\lvert X_c \rvert}{Sin\theta}$
D	Loss coefficient/Dissipation Factor	$tan\delta = \frac{ESR}{X_c}$
Rs	Equivalent Series Resistance	$ESR = \lvert Z \rvert Cos\theta$

5. Proposed Deep Learning Model

This study offers a robust condition-monitoring framework for the aluminium electrolytic capacitors found in SMPS. These capacitors are smoothing devices to achieve the required voltage for SMPS applications. The primary goal of this research is to identify defects among these capacitors with different capacities of 2200uf, 1000uf, and 470uf, utilizing a multi-parametric data acquisition method to gather information on capacitance (Cp), impedance (Z), dissipation factor (DF), and equivalent series resistance (ESR).

The datasheet for every capacitor contains the functional parameters that guarantee their working conditions. We have examined the stability of the capacitors in cold environments in line with the

Preprints (www.preprints.org) | NOT PEER-REVIEWED | Posted: 20 July 2023 doi:10.20944/preprints202307.1373.v1

manufacturer's recommendations. The expected working environment for the capacitors is not meant to be below - 40 ° C. The primary sensitivity to temperature of the capacitors is the higher frequency hence the deployment of the LCR as the data acquisition tool. The frequency range for the LCR meter is from 4Hz to 8MHz, so we have exposed the capacitors to the highest range (8MHz). These have assisted in exposing the capacitors for a longer period and ensuring the right amount of data for further analysis. The data preprocessing steps and feature engineering are the next focus after the data collection process. Time domain features were extracted from the 2200uf, 1000uf and 470uf capacitor datasets. Interestingly, we adopted the Pearson correlation coefficient with a threshold of 0.9 to select the meaningful features across the capacitors. The result is concatenated, normalized, scaled and labelled before feeding to the ANN classifier for training and testing. The overall architecture of the ANN proposed model is shown in Figure 2. The adopted parameters for the ANN model is shown in Table 3 comprising of the hidden layers, activation, learning rate, validation setting, solver function, random state value, and the iteration value.

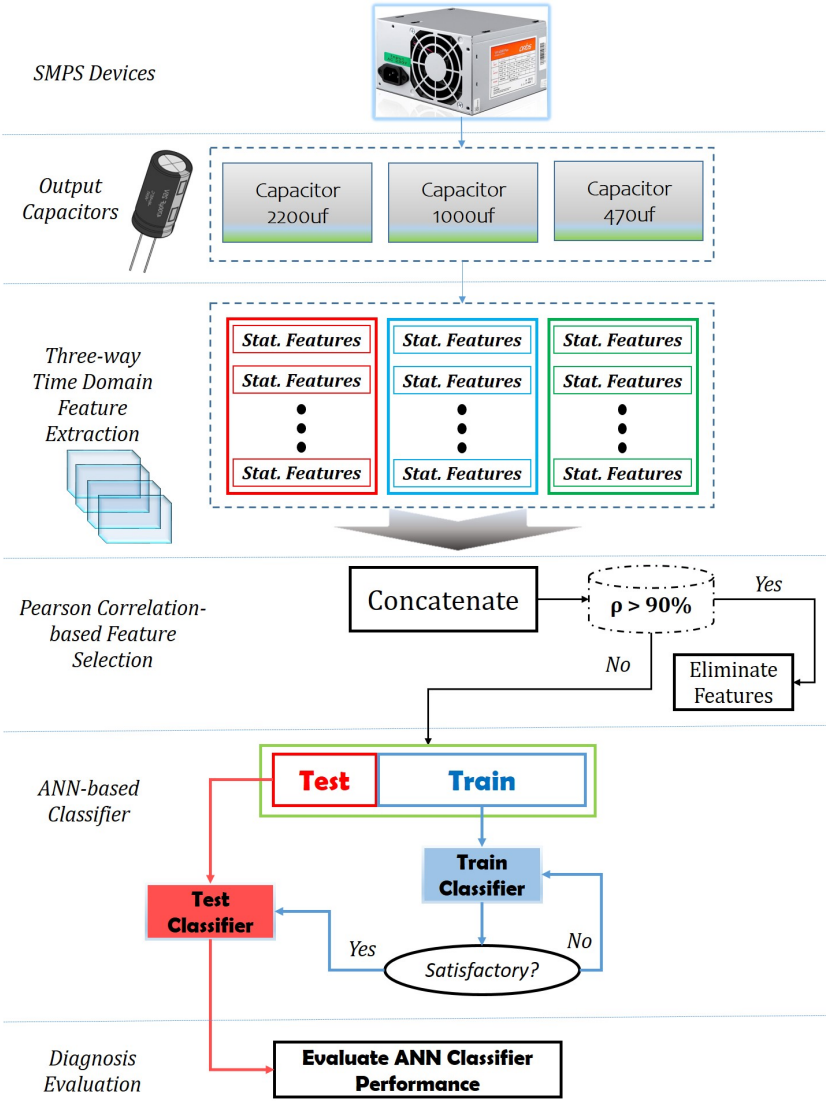

Figure 2. Proposed ANN-based Fault Diagnosis Framework

Preprints (www.preprints.org) | NOT PEER-REVIEWED | Posted: 20 July 2023 doi:10.20944/preprints202307.1373.v1

Table 3. ANN-Classifier Model Parameters

Parameters	Values
Hidden Layer Size	25
Max-iter	50
Activation	reLu
Solver	Adam
Random state	1
Early stopping	True
Validation Fraction	0.2
Learning rate	0.001

5.1. Statistical Feature Engineering

Aluminium electrolytic capacitors generate time-dependent electrical signals. Pearson correlation helps analyze the temporal relationship between signals, identifying lagged correlations and dependencies. Time series analysis using Pearson correlation aids in anticipating capacitor behaviour, calculating remaining useful life, and understanding the impact of age or temperature. Pearson correlation is a mathematical measure to evaluate relationships in the context of electrical signals from aluminium electrolytic capacitors. It evaluates the inter-dependencies between these features, separating significant connections from weak correlations. Understanding the properties and behaviour of capacitors is vital for studying their electrical signals, aiding in fault identification, quality control, and anomaly detection. Table 4 shows the time-domain features extracted from the set of aluminium electrolytic capacitors, which are 14 in number and namely, root mean square, mean, kurtosis, interquartile range, median abs deviation, skewness, Max, Min, crest factor, peak factor, wave factor, standard error mean, standard deviation, and variance.

Table 4. The Definitions of the Statistical Features Extracted.

Feature Description	Definitions
Root Mean Square	$X_{rms} = \sqrt{\frac{\sum_{i=1}^{n}(x_i)^2}{n}}$
Mean	$\bar{x} = \frac{1}{n}\left(\sum_{i=1}^{n} x_i\right)$
Kurtosis	$X_{kurt} = \frac{1}{N}\Sigma\left(\frac{(x_i-\mu)^3}{\sigma}\right)$
Interquartile range	$upperquarterQ_3 - lowerquarterQ_1$
Median abs deviation	$X_{mad} = \frac{1}{n}\sum_{i=1}^{n}\lvert x_i - m\rvert$
Skewness	$X_{\text{skew}} = E\left[\left(\frac{(x_i-\mu)^3}{\sigma}\right)\right]$
Max	$X_{\max} = \max\left(x_i\right)$
Min	$X_{\max} = \min\left(x_i\right)$
Crest Factor	$X_{CF} = \frac{x_{\max}}{x_{rms}}$
Peak factor	$x_{PF} = \frac{x_{\max}}{\sqrt{x_s}}$
Wave Factor	$x_{WF} = \frac{\sqrt{\frac{1}{n}\sum_{i=1}^{n}\lvert x_i\rvert^2}}{\frac{1}{n}\sum_{i=1}^{n}\lvert x_i\rvert}$
Standard error mean	$X_{sem} = \frac{standarddeviation}{\sqrt{n}}$
Standard deviation	$SD = \sqrt{\frac{1}{N-1}\sum_{i=1}^{N}(x_i - \bar{x})^2}$
Variance	$VAR = \sqrt{\frac{1}{N}\sum_{i=1}^{N}(x_i - \bar{x})^2}$

Preprints (www.preprints.org) | NOT PEER-REVIEWED | Posted: 20 July 2023 doi:10.20944/preprints202307.1373.v1

The feature extraction visualization was not included due to the space constraint. Figure 3, 4, 5, 6, 7 shows the feature selection visualization plot for the set of capacitors using the impedance parameter as a standalone under varying temperatures. The resulting features are as follows: mean, variance, interquartile range, maximum, median absolute deviation, kurtosis, skewness, crest factor, wave factor, and peak factor. It can be noted that the feature selection plot for the - 40 ° C of the capacitors added wave factor to its result compared to the other four temperature ranges, as shown in Figure 7. It can be deduced at - 20 ° C as shown in Figure 5 that the selected features fall within the range of 0.25 to 0.75, which signifies a turning point for the capacitor health before it stabilizes back at - 30 ° C.

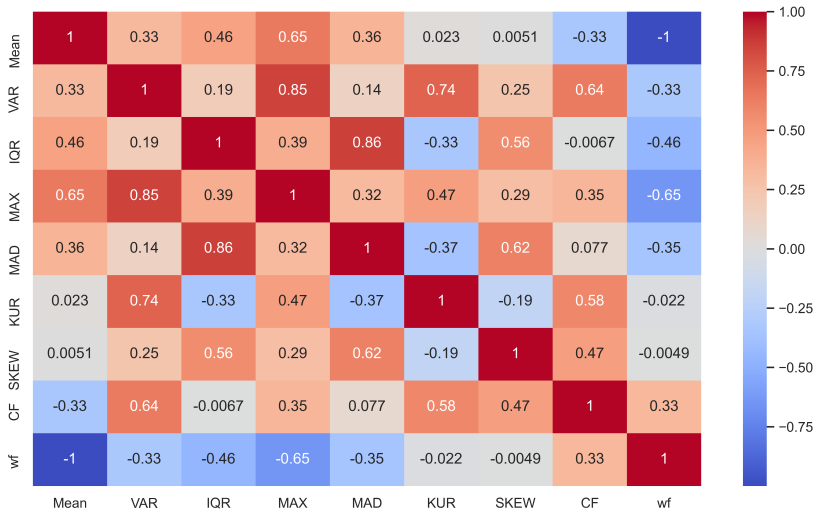

Figure 3. Visualization of Feature Selection at -5 ° C: Uncovering Discriminant Information for Enhanced Data Analysis.

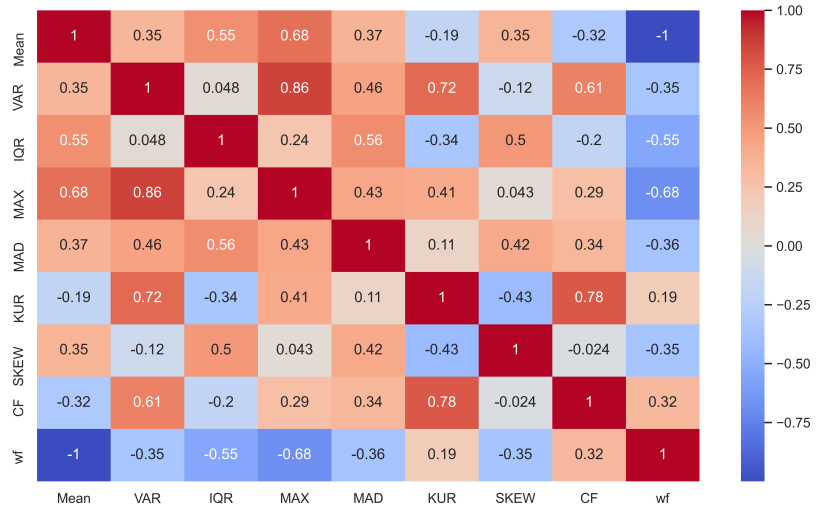

Figure 4. Visualization of Feature Selection at -10 ° C: Uncovering Discriminant Information for Enhanced Data Analysis.

Preprints (www.preprints.org) | NOT PEER-REVIEWED | Posted: 20 July 2023 doi:10.20944/preprints202307.1373.v1

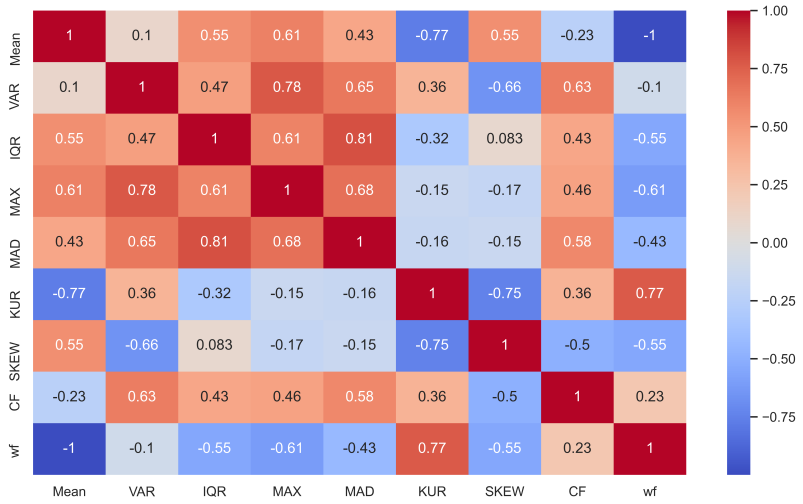

Figure 5. Visualization of Feature Selection at -20 ° C: Uncovering Discriminant Information for Enhanced Data Analysis.

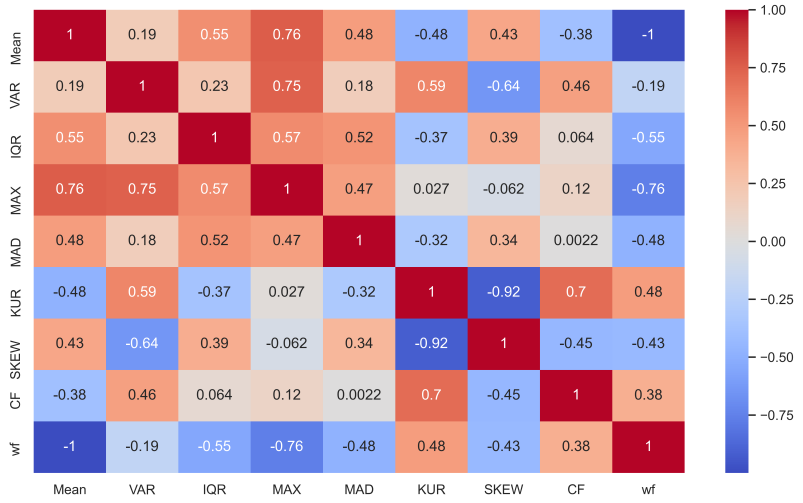

Figure 6. Visualization of Feature Selection -30 ° C: Uncovering Discriminant Information for Enhanced Data Analysis.

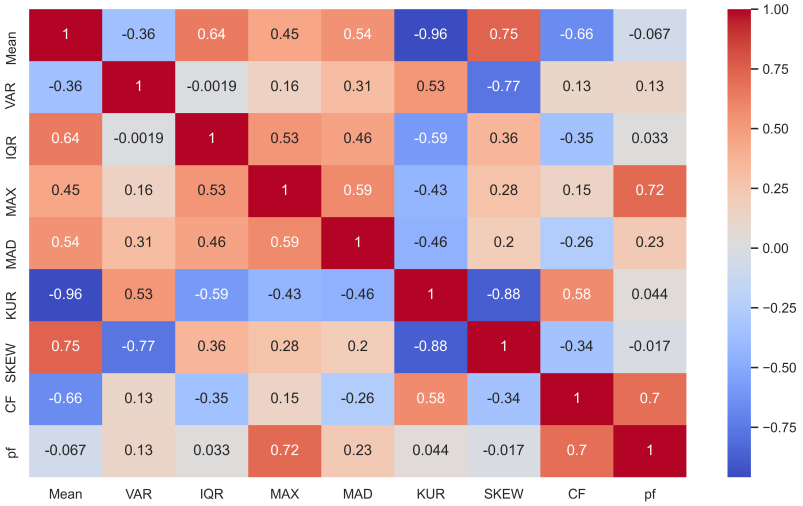

Figure 7. Visualization of Feature Selection at -40 ° C: Uncovering Discriminant Information for Enhanced Data Analysis.

Preprints (www.preprints.org) | NOT PEER-REVIEWED | Posted: 20 July 2023 doi:10.20944/preprints202307.1373.v1

6. Result Analysis and Discussion

Following identifying the distinguishing features through the utilization of the correlation coefficient, the categorized dataset was divided for training and testing using the ratio 70/30 (70 per cent for training and 30 per cent for testing). However, 20 per cent of the dataset was allocated for model validation. Cross-validation was employed during the training of the Artificial Neural Network (ANN) classifiers to address overfitting and ensure precise performance measurements. This process entails dividing the dataset into multiple subsets or folds. The ANN model is then trained on a combination of these folds while being evaluated on the remaining fold. This procedure is repeated several times, with each fold serving as a training and validation set. By rotating the folds, cross-validation permits a comprehensive evaluation of the model across the entire dataset, minimizing the risk of overfitting. Accuracy, precision, recall, and F1 score are performance metrics computed by aggregating the outcomes from each iteration, providing a dependable estimate of the classifier's performance on unseen data [38–41]. Interestingly, we implemented the k-fold cross-validation technique to prevent overfitting with k set to five. ANN classification performance metrics are utilized to evaluate the precision and efficiency of the network in predicting class labels for a given dataset. The mathematical expression is as follows:

$$\text{Accuracy} = \frac{TP}{TP + FP + TN + FN} \tag{3}$$

$$\text{Recall/Sensitivity} = \frac{TP}{TP + FN} \tag{4}$$

$$\text{Precision} = \frac{TP}{TP + FP} \tag{5}$$

$$\text{F1- Score} = \frac{2 * \text{Sensitivity} * \text{Precision}}{\text{Precision} + \text{sensitivity}} \tag{6}$$

where, TP = True Positive, TN = True Negative, FP = False Positive, and FN = False Negative.

Table 5. Global performance under varying temperature and electrical parameters

Fault Classification	Electrical Parameters	Accuracy (%)	Precision (%)	Recall (%)	F1-Score (%)	Cost (s)
- 5 ° C	Capacitance	42.22	49.93	42.22	38.55	6.0333
	Impedance	**98.44**	**100.00**	**100.00**	**100.00**	**9.9200**
	DF	40.69	40.00	40.69	38.18	5.3000
	ESR	83.74	84.74	83.75	83.42	9.4333
- 10 ° C	Capacitance	49.44	56.03	49.44	49.28	8.3800
	Impedance	**92.50**	**93.52**	**92.50**	**92.40**	**11.1000**
	DF	32.36	10.47	32.36	15.83	2.4733
	ESR	76.52	78.65	76.53	76.51	5.4400
- 20 ° C	Capacitance	46.11	43.39	46.11	43.70	8.0933
	Impedance	**69.72**	**73.65**	**69.72**	**67.94**	**9.4400**
	DF	57.64	64.35	57.64	58.16	9.3867
	ESR	57.78	58.09	57.78	56.94	7.3867
- 30 ° C	Capacitance	69.30	69.48	69.31	68.57	7.5267
	Impedance	**97.91**	**98.07**	**97.92**	**97.91**	**10.7333**
	DF	61.94	63.50	61.94	61.83	9.6067
	ESR	76.52	77.34	76.53	76.17	8.4800
- 40 ° C	Capacitance	54.58	58.07	54.58	48.06	7.0200
	Impedance	**88.75**	**90.96**	**88.75**	**88.84**	**11.0133**
	DF	59.58	62.04	59.58	59.73	6.4000
	ESR	74.58	75.49	74.58	73.89	9.6000

Table 5 shows the performance metrics in evaluating the aluminium electrolytic capacitors under varying temperatures. We have used a Pearson correlation coefficient in selecting and quantifying the fault patterns between the electrical signals of the capacitors. The main objective of this study is

Preprints (www.preprints.org) | NOT PEER-REVIEWED | Posted: 20 July 2023 doi:10.20944/preprints202307.1373.v1

to select the best candidate among the electrical signals that can show distinguishable diagnostics characteristics to classify the faults in the capacitor. The impedance signal shows a better trend in terms of the features selected and performance metrics among the candidate for electrical signals. Exposing the capacitors to a range of cold temperatures shows a trend in the accuracy of the diagnostics result. At the lowest cold region, the capacitors had an accuracy of 98.44% with a computational cost of 9.9200 seconds compared to the highest cold region with an accuracy figure of 88.75% with a computational cost of 11.0133 seconds. On one hand, the impedance signal is a better candidate for the capacitor diagnostics tool at both lower and high cold regions compared to the other signals.

Figure 8 shows the histogram plot to visualize the comprehensive analysis of the assessment of the model put together. The plot legend shows the capacitance, impedance, dissipation factor and ESR with blue, orange, green and red colours, respectively. The impedance signal was able to provide diagnostic features across all the temperature variances compared to the other electrical signals. However, the performance of the capacitor declined to an average of 57.81% at - 20 ° C. In comparison between the - 5 ° C and - 40 ° C, the accuracy of the impedance signal dropped by 9.69%. This result shows the capacitor declining in its performance at the peak of the temperature compared to the lowest cold region (- 5 ° C). Also, there was an above-average performance by the ESR signal at varying temperatures. The ESR is a great contender as a diagnostic tool for AEC owing to different research methodologies. However, it falls short under the influence of temperature in this study. There is existing research that supports the decrease in the value of the capacitance under extremely low temperatures and an increase under extremely high temperatures. The result from this study, supports the existing results in this regard, as it could not be picked as a diagnostic tool for the capacitor based on its below-average accuracy result.

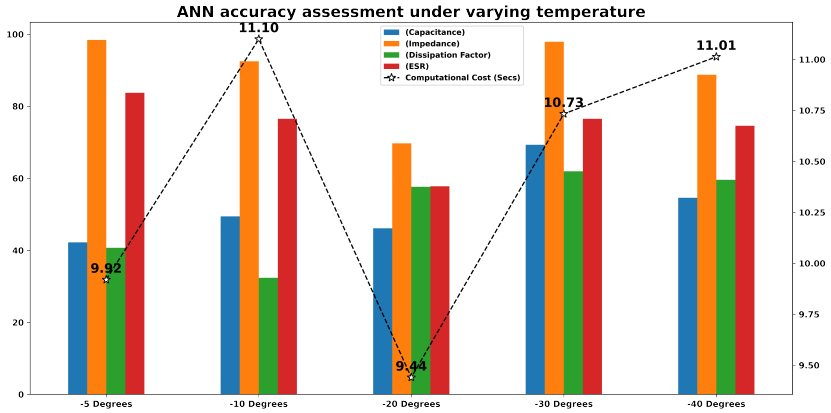

Figure 8. ANN Accuracy Assessment under varying temperature and electrical parameters

Figure 9 shows the confusion matrix fault samples of - 5 °C. The label 0, 1, and 2 on the confusion matrix corresponds to the capacitor sample 2200uf, 1000uf and 470uf, respectively. Among the 245 samples labelled as 0, 244 were predicted accurately, and 1 sample was predicted as labelled 1. Out of 242 samples for label 1, it predicted 241 samples correctly and 1 sample inaccurately as 0 label. Label 2 was predicted accurately by the model resulting in 233 samples. Figure 10 shows the confusion matrix fault samples of - 40 °C. Among the 245 samples for the 0 label, 229 were predicted correctly, while 14 and 2 samples were predicted as labels 1 and 2, respectively. Among the 242 samples for the 1 label, 241 were predicted correctly, and 1 sample was predicted as label 2. Among the 232 samples for the 2 label, 209 were predicted correctly, and 24 samples were predicted as label 1. Overall, the outcome of this study is the accurate condition monitoring of the aluminium electrolytic capacitors found in SMPS using the Pearson correlation coefficient and the ANN model.

Preprints (www.preprints.org) | NOT PEER-REVIEWED | Posted: 20 July 2023 doi:10.20944/preprints202307.1373.v1

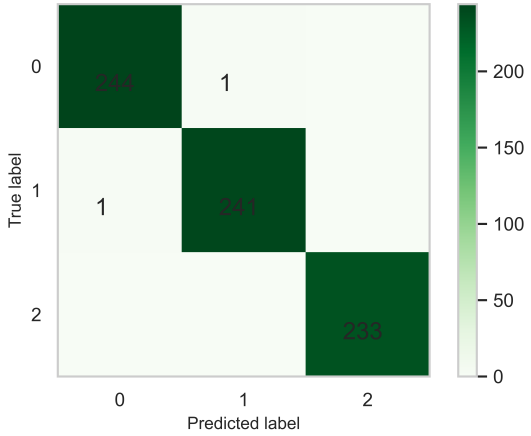

Figure 9. Confusion Matrix Results of Artificial Neural Network (ANN) for - 5 °C Capacitor Classification Fault Diagnostics.

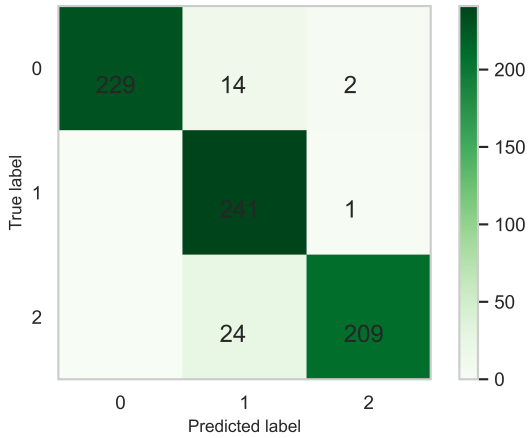

Figure 10. Confusion Matrix Results of Artificial Neural Network (ANN) for - 40 °C Capacitor Classification Fault Diagnostics.

7. Conclusions

The behaviour of an aluminium electrolytic capacitor was specifically examined in this experiment-based research paper's focus on switched-mode power supplies (SMPS). The failure mode effect analysis of the capacitor revealed its vulnerability to defects, which served as the driving force behind this investigation. The experiment exposed the capacitor to temperatures between -5 and - 40 ° C to evaluate how it would react in a cold environment. The equivalent series resistance (ESR), impedance, dissipation factor, and capacitance were all measured using an LCR meter. These properties were measured at various temperatures to capture the capacitor's behaviour over the cold range. An Artificial Neural Network (ANN) classifier was used for classification and analysis. The gathered data were used to train and test the ANN model. After careful examination, it was discovered that impedance (Z), among the measured characteristics for the three output capacitors under inquiry, showed the greatest accuracy (98.44% and 88.75%) across the range of temperatures at -5 and - 40 ° C respectively. The results underline that impedance is important as a reliable gauge of the capacitor's performance, particularly in cold conditions. These results can improve the reliability and efficiency of SMPS applications, which can also help in fault detection and monitoring systems for such capacitors. The effects of additional environmental conditions, such as high temperatures or humidity, on capacitor behaviour might be explored in more detail, and the relationship between variations in impedance and certain capacitor failure types could be examined. For future works, we

would explore the remaining useful life approach by exceeding the temperature benchmark set by the manufacturer of the capacitors.

Author Contributions: Conceptualization, S.J. and A.B.K.; methodology, S.J. and A.B.K.; software, S.J. and A.B.K.; and J.-W.H.; validation, A.B.K.; formal analysis, A.B.K.; investigation, S.J.; S.S. and A.B.K.; data curation, S.J. and S.S.; writing—original draft preparation, A.B.K.; writing—review and editing, A.B.K.; visualization, S.J. and A.B.K.; resources and supervision, J.-W.H.; project administration, J.-W.H.; funding acquisition, J.-W.H. All authors have read and agreed to the published version of the manuscript.

Funding: This research was supported by the MSIT (Ministry of Science and ICT), Korea, under the Grand Information Technology Research Center support program (IITP–2023–2020–0–01612), supervised by the IITP (Institute for Information and communications Technology Planning and Evaluation).

Data Availability Statement: The data presented in this study are available on request from the corresponding author. The data are not publicly available due to laboratory regulations.

Conflicts of Interest: The authors declare no conflicts of interest.

References

1. Kareem, A.B.; Hur, J.-W. A Feature Engineering-Assisted CM Technology for SMPS Output Aluminium Electrolytic Capacitors (AEC) Considering D-ESR-Q-Z Parameters. *Processes* **2022**, *10*, 1091. https://doi.org/10.3390/pr10061091
2. Jami T., Charles J., Ali S., Electrolytic capacitor: Properties and operation, *Journal of Energy Storage*, **2023** *Volume 58*, 106330, ISSN 2352-152X, https://doi.org/10.1016/j.est.2022.106330.
3. Shahraki, A. F., Al-Dahidi, S., Taleqani, A. R., and Yadav, O. P. Using LSTM neural network to predict the remaining useful life of electrolytic capacitors in dynamic operating conditions. *Journal of Risk and Reliability*, **2023**, *237(1)*, 16-28, https://doi.org/10.1177/1748006X221087.
4. Duan, C. and Chen, P. "Adaptive Maintenance Scheme for Degrading Devices With Dynamic Conditions and Random Failures," in *IEEE Transactions on Industrial Informatics*, *vol. 19*, no. 3, pp. 2508-2519, **2023**, doi: 10.1109/TII.2022.3182789.
5. Wang, Y.; Wu, T.; Che, L.; Huang, G. Microstructure and Recrystallization Behavior of Heating Rate-Controlled Electrolytic Capacitor Aluminum Foil under Cold Forming and Annealing. *Materials* **2023**, *16*, 4128. https://doi.org/10.3390/ma16114128
6. Banerjee, R. John, D. Zhang, C. Agarwal, A. and Raj, P. "Cold-sprayed aluminium capacitors on lead frames for 3D power packaging," *2023 Fourth International Symposium on 3D Power Electronics Integration and Manufacturing (3D-PEIM)*, Miami, FL, USA, **2023**, pp. 1-4, doi: 10.1109/3D-PEIM55914.2023.10052633.
7. Both, J. "The modern era of aluminium electrolytic capacitors," in *IEEE Electrical Insulation Magazine*, *vol. 31*, no. 4, pp. 24-34, **2015**, doi: 10.1109/MEI.2015.7126071.
8. Yao, B, Zhao, S., Zhang, Y., and Wang, H. "A Health Indicator of Aluminum Electrolytic Capacitors Based on Strain Sensing," in *IEEE Transactions on Power Electronics*, **2023** *vol. 38*, no. 7, pp. 7982-7987, doi: 10.1109/TPEL.2023.3263125.
9. Suskis, P., Zakis, J., Suzdalenko, A., Van Khang H., and Pomarnacki, R. "A Study on Electrolytic Capacitor Aging in Power Converters and Parameter Change Over the Lifespan," *2023 IEEE 10th Jubilee Workshop on Advances in Information, Electronic and Electrical Engineering (AIEEE), Vilnius, Lithuania*, **2023**, pp. 1-5, doi: 10.1109/AIEEE58915.2023.10135053.
10. Wei, Y., Hossain, M. and Mantooth, H. A. "Evaluation and Modeling of SiC Based Power Converter for Low-Temperature Operation," in *IEEE Transactions on Industry Applications*, **2023** *vol. 59*, no. 3, pp. 3660-3673, doi: 10.1109/TIA.2023.3247404.
11. Suchong T., Han Y., Zhen Z., Xiangyu X., Yuanyuan X., Jian Z., Xinchi Z., Zhengdao P., Xingyou R., Yudong G., Zhoulu W., Yutong W., Xiang L., and Yi Z., The Progress of Hard Carbon as an Anode Material in Sodium-Ion Batteries, *Molecules*, **2023**, *28*, 7, (3134), doi: 10.3390/molecules28073134.
12. Xian Z., Jiatong B., Libo L., Qian C., Li L., Xiangxiang C., Youyuan W., Xuanyu X., and Guoliang X., Preparation and characterization of an anode foil for aluminium electrolytic capacitors by powder additive manufacturing, *Powder Technology*, *Volume 426*, **2023**, 118602, ISSN 0032-5910, https://doi.org/10.1016/j.powtec.2023.118602.

13. Cousseau, R., Patin, N., Monmasson, E. and Idkhajine, L. "A methodology for studying aluminium electrolytic capacitors wear-out in automotive cases," *2013 15th European Conference on Power Electronics and Applications (EPE), Lille, France* **2013**, pp. 1-10, doi: 10.1109/EPE.2013.6631846.
14. Bhargava, C., Banga, V.K. and Singh, Y. "Condition monitoring of aluminium electrolytic capacitors using accelerated life testing: A comparison", *International Journal of Quality and Reliability Management*, **2018**, *Vol. 35* No. 8, pp. 1671-1682. https://doi.org/10.1108/IJQRM-06-2017-0115.
15. Amaral, A. M. R. and Cardoso, A. J. M. "Using Newton-Raphson Method to Estimate the Condition of Aluminum Electrolytic Capacitors," *2007 IEEE International Symposium on Industrial Electronics, Vigo, Spain* **2007**, pp. 827-832, doi: 10.1109/ISIE.2007.4374704.
16. Jedtberg, H., Buticchi, G., Liserre, M., and Wang, H. A method for hotspot temperature estimation of aluminium electrolytic capacitors. *2017 IEEE Energy Conversion Congress and Exposition (ECCE), OH, USA* **2017**, pp. 3235-3241, doi: 10.1109/ECCE.2017.8096586.
17. Kareem, A.B.; Hur, J.-W. Towards Data-Driven Fault Diagnostics Framework for SMPS-AEC Using Supervised Learning Algorithms. *Electronics* **2022**, *11*, 2492. https://doi.org/10.3390/electronics11162492.
18. Bărbulescu, C.; Căiman, D.-V.; Dragomir, T.-L. Parameter Observer Useable for the Condition Monitoring of a Capacitor. *Appl. Sci.* **2022**, *12*, 4891. https://doi.org/10.3390/app12104891.
19. Zhou, Y., Liao, R. and Chen, Y. "Study on Optimization of Data-Driven Anomaly Detection," *2022 International Conference on Data Science and Its Applications (ICoDSA), Bandung, Indonesia*, **2022**, pp. 123-127, doi: 10.1109/ICoDSA55874.2022.9862914.
20. Okwuosa, C.N.; Hur, J.-w. A Filter-Based Feature-Engineering-Assisted SVC Fault Classification for SCIM at Minor-Load Conditions. *Energies* **2022**, *15*, 7597. https://doi.org/10.3390/en15207597.
21. Kareem, A.B.; Ejike Akpudo, U.; Hur, J.-W. An Integrated Cost-Aware Dual Monitoring Framework for SMPS Switching Device Diagnosis. *Electronics* **2021**, *10*, 2487. https://doi.org/10.3390/electronics10202487.
22. Laadjal, K.; Bento, F.; Cardoso, A.J.M. On-Line Diagnostics of Electrolytic Capacitors in Fault-Tolerant LED Lighting Systems. *Electronics* **2022**, *11*, 1444. https://doi.org/10.3390/electronics11091444.
23. Amaral, A.M.R.; Laadjal, K.; Cardoso, A.J.M. Advanced Fault-Detection Technique for DC-Link Aluminum Electrolytic Capacitors Based on a Random Forest Classifier. *Electronics* **2023**, *12*, 2572. https://doi.org/10.3390/electronics12122572.
24. Zhou, X.; Han, X.; Wang, Y.; Lu, L.; Ouyang, M. A Data-Driven LiFePO4 Battery Capacity Estimation Method Based on Cloud Charging Data from Electric Vehicles. *Batteries* **2023**, *9*, 181. https://doi.org/10.3390/batteries9030181.
25. Iqbal, T.; Elahi, A.; Wijns, W.; Amin, B.; Shahzad, A. Improved Stress Classification Using Automatic Feature Selection from Heart Rate and Respiratory Rate Time Signals. *Appl. Sci.* **2023**, *13*, 2950. https://doi.org/10.3390/app13052950.
26. Cen, S.; Yoo, J.H.; Lim, C.G. Electricity Pattern Analysis by Clustering Domestic Load Profiles Using Discrete Wavelet Transform. *Energies* **2022**, *15*, 1350. https://doi.org/10.3390/en15041350.
27. Viswa Teja, A.; Razia Sultana, W.; Salkuti, S.R. Performance Explorations of a PMS Motor Drive Using an ANN-Based MPPT Controller for Solar-Battery Powered Electric Vehicles. *Designs* **2023**, *7*, 79. https://doi.org/10.3390/designs7030079.
28. Oyedeji, M.O.; Alharbi, A.; Aldhaifallah, M.; Rezk, H. Optimal Data-Driven Modelling of a Microbial Fuel Cell. *Energies* **2023**, *16*, 4740. https://doi.org/10.3390/en16124740.
29. Kim, T.-G.; Lee, H.; An, C.-G.; Yi, J.; Won, C.-Y. Hybrid AC/DC Microgrid Energy Management Strategy Based on Two-Step ANN. *Energies* **2023**, *16*, 1787. https://doi.org/10.3390/en16041787.
30. Jlidi, M.; Hamidi, F.; Barambones, O.; Abbassi, R.; Jerbi, H.; Aoun, M.; Karami-Mollaee, A. An Artificial Neural Network for Solar Energy Prediction and Control Using Jaya-SMC. *Electronics* **2023**, *12*, 592. https://doi.org/10.3390/electronics12030592.
31. Jasim, A.M.; Jasim, B.H.; Neagu, B.-C.; Alhasnawi, B.N. Coordination Control of a Hybrid AC/DC Smart Microgrid with Online Fault Detection, Diagnostics, and Localization Using Artificial Neural Networks. *Electronics* **2023**, *12*, 187. https://doi.org/10.3390/electronics12010187.
32. Sankar, R.S.R.; Deepika.K, K.; Alsharef, M.; Alamri, B. A Smart ANN-Based Converter for Efficient Bidirectional Power Flow in Hybrid Electric Vehicles. *Electronics* **2022**, *11*, 3564. https://doi.org/10.3390/electronics11213564.

33. P. Suskis, J. Zakis, A. Suzdalenko, H. Van Khang and R. Pomarnacki, "A Study on Electrolytic Capacitor Aging in Power Converters and Parameter Change Over the Lifespan," *2023 IEEE 10th Jubilee Workshop on Advances in Information, Electronic and Electrical Engineering (AIEEE), Vilnius, Lithuania*, **2023**, pp. 1-5, doi: 10.1109/AIEEE58915.2023.10135053.
34. Metsämuuronen, J. Artificial systematic attenuation in eta squared and some related consequences: attenuation-corrected eta and eta squared, negative values of eta, and their relation to Pearson correlation. *Behaviormetrika*, **2023** *50*, 27–61. https://doi.org/10.1007/s41237-022-00162-2.
35. Denuit, M., Trufin, J. Model selection with Pearson's correlation, concentration and Lorenz curves under autocalibration. *Eur. Actuar. J.*, **2023** https://doi.org/10.1007/s13385-023-00353-5.
36. Yücelbaş, C. and Yücelbaş, Ş. Examining the Success of Information Gain, Pearson Correlation, and Symmetric Uncertainty Ranking Methods on 3D Hand Posture Data for Metaverse Systems. *Sakarya University Journal of Science*, **2023**, *27* (2), 271-284, DOI: 10.16984/saufenbilder.1206968.
37. Wan, Z. Analysis and Prediction of Wordle Dataset Based on ARIMA and Pearson's Correlation Coefficient. *Frontiers in Computing and Intelligent Systems*, **2023**, *3(2)*, 39–43. https://doi.org/10.54097/fcis.v3i2.7082.
38. Cunha, F.; Ribeiro, T.; Lopes, G.; Ribeiro, A.F. Large-Scale Tactile Detection System Based on Supervised Learning for Service Robots Human Interaction. *Sensors* **2023**, *23*, 825. https://doi.org/10.3390/s23020825.
39. Fuadah, Y.N.; Pramudito, M.A.; Lim, K.M. An Optimal Approach for Heart Sound Classification Using Grid Search in Hyperparameter Optimization of Machine Learning. *Bioengineering* **2023**, *10*, 45. https://doi.org/10.3390/bioengineering10010045.
40. Soomro, A.A.; Mokhtar, A.A.; Salilew, W.M.; Abdul Karim, Z.A.; Abbasi, A.; Lashari, N.; Jameel, S.M. Machine Learning Approach to Predict the Performance of a Stratified Thermal Energy Storage Tank at a District Cooling Plant Using Sensor Data. *Sensors* **2022**, *22*, 7687. https://doi.org/10.3390/s22197687.
41. Amin, M.N.; Ahmad, A.; Khan, K.; Ahmad, W.; Nazar, S.; Faraz, M.I.; Alabdullah, A.A. Split Tensile Strength Prediction of Recycled Aggregate-Based Sustainable Concrete Using Artificial Intelligence Methods. *Materials* **2022**, *15*, 4296. https://doi.org/10.3390/ma15124296.